体スーパーファミリーのリガンドとして、2005年までにヒトで18種類の分子が確認されている。これらの分子群は、受容体からの細胞内シグナルによってその機能が発揮され、細胞死を誘導する以外にも、免疫細胞の活性化などを誘導することが知られている。そこで本研究では、免疫活性化能を有するTNFsfに焦点をしぼり、安全性・有効性に優れた粘膜ワクチンアジュバントを創製するための基礎検討を行い、HIVに対する粘膜ワクチンアジュバントの開発を試みるものである。

**B. 研究方法**

アジュバント

コレラトキシンBサブユニット（CT-B）は、List Biological Laboratory（Campbell, CA）より購入した。16種類のTNF superfamily（TNFsf: human APRIL, mouse BAFF, mouse 4-1BBL, mouse CD27L, mouse CD30L, mouse CD40L, mouse EDA, mouse GITRL, mouse LIGHT, mouse LT-α, mouse OX40L, mouse TL1A, mouse TNF-α, mouse TRAIL, mouse TRANCE, mouse TWEAK)は、R&D社（Minneapolis, MN）より購入した。

免疫方法

BALB/cマウス（6～8週齢、雌性）への経鼻免疫は、個々のTNFsfあるいはCT-Bをニワトリ卵白アルブミン（OVA；SIGMA）と混合投与し、非麻酔条件下で行なった。尚、投与スケジュールは1週間間隔で3回行った。

サンプル回収

1) 血清サンプルの回収；最終免疫から1週間後に眼底採血を行い、11000 rpm、10分遠心操作を行うことにより血清を回収した。
2) 鼻腔洗浄液の回収；マウス鼻腔内を200 μL PBSで洗浄後、14000 rpm、20分、4 °C遠心操作を行うことにより鼻腔洗浄液を調製した。
3) 膣洗浄液の回収；マウス膣腔内を100 μL PBSで洗浄後、14000 rpm、20分、4 °C遠心操作を行うことにより膣洗浄液を調製した。
4) 糞便抽出液の調製；100 mg/mLとなるようにPBSを加え、4 °C、2時間激しく撹拌した。得られた懸濁液を14000 rpm、4 °C、20分遠心し、上清を回収して糞便抽出液を調製した。

OVA特異的抗体産生能の評価（OVA specific Ig ELISA）

OVA（10 μg/mL、in 50 mM Bicarbonate Buffer）をELISAプレートに加え、4 °Cで一晩放置し固相した。PBSで2倍希釈したBlock Aceを室温で1時間反応させることでブロッキング後、各濃度に調製したサンプルを加えて反応させた（IgG; 室温、2時間、IgA; 37 °C、2時間）。これらのプレートを0.05% Tween含有PBSあるいは、0.05% Tween含有TBSで洗浄後、各濃度に調製したHRP標識IgG抗体およびビオチン標識IgA抗体を加えて反応させた（IgG; 室温、2時間、IgA; 37 °C、2時間）。IgAの測定では、プレート洗浄後、1/2500に希釈したHRP標識ストレプトアビジンを加え、室温で1時間反応させた。再度、洗浄操作を行い最後に蒸留水で洗浄した後、TMBZ基質液を添加した。2N $H_2SO_4$を添加することにより発色反応を停止させ、測定波長450 nm、参考波長690 nmにおける吸光度を測定した。

脾細胞の調製方法

最終免疫7日後のマウスから脾臓を無菌的に摘出した後、70 μmセルストレーナー上で細胞を分散させ、1500 rpm、5 min、4 °Cの条件で遠心することで、細胞のペレットを回収した。回収したペレットをRPMI 1640（10% FBS、50 μM 2-ME、抗生物質を含む）で洗浄操作を1回行った後、$NH_4Cl$溶液で懸濁することにより赤血球を除去した。さらに遠心操作を行った後、RPMI 1640（10% FCS、50 μM 2-ME、10 mL/L of a 100x non-essential amino acids solution、1 mM sodium pyruvate、10 mM HEPES）で懸濁し、脾細胞を調製した。

Bio-Plex Multiplex Cytokine assay

マウスから回収した脾細胞を$5 \times 10^6$ cells/wellで24 well plateフィルタープレートに播種し、OVA溶液

を終濃度 1 mg/mL となるように添加し、37 °C で 72 時間培養した。Cytokine assay buffer を添加してフィルターを馴染ませた後、1 次抗体付きビーズ溶液および Cytokine assay buffer を添加した。その後、培養上清を添加し、300 rpm で攪拌しながら室温で 30 分インキュベートした。洗浄操作を 3 回行った後、detection antibody を添加し、300 rpm で攪拌しながら室温で 30 分インキュベートした。3 回洗浄操作を行った後、PE 標識 streptavidin を添加し、300 rpm で攪拌しながら室温で 10 分インキュベートした。3 回の洗浄操作を行った後、Cytokine assay buffer で beads を懸濁し、Bio-Plex system により、サイトカイン産生（IL-2、IL-4、IL-5、IL-10、IL-12、GM-CSF、IFN-γ、TNF-α）を測定した。

IFN-γ ELISPOT assay

マウスから回収した脾細胞を $5 \times 10^6$ cells/well で 96 well ELISPOT plate に播種し、OVA 溶液を終濃度 1 mg/mL となるように添加し、37 °C で 24 時間培養した。96 well ELISPOT plate に capture antibody を添加して PVDF 膜に 4 °C で一晩固相化した。Capture antibody の除去後、blocking solution を添加して室温で 2 時間インキュベートした。さらに、OVA を最終濃度が 1 mg/mL となるように添加した後、脾細胞を $5 \times 10^6$ cells/well となるように ELISPOT plate に添加した。37 °C で培養した後、脾細胞を除去し、蒸留水および PBST で洗浄操作を 2 回繰り返した。その後、Detection antibody および streptavidin-HRP を添加した後、substrate solution を添加して室温で 30 分インキュベートし、発色の程度をモニタリングした。蒸留水を加えることにより、発色反応を停止させ、室温で 2 時間から一晩かけて乾燥させた。スポット数の計測は、KS ELISPOT イメージングシステムを用いて行なった。

**C. 研究結果**

本分担研究では、HIV の感染防御を目的とした粘膜ワクチンの開発のため、医薬価値に優れたサイトカインを、安全性・有効性に優れた粘膜ワクチンアジュバントへ適用するための基礎検討を行った。本年度は、生体防御に関わるサイトカインの中から、免疫活性化能に優れたサイトカインスーパーファミリーの一つである TNFsf に焦点を絞り、TNFsf の中から、粘膜ワクチンアジュバント活性に優れた分子をスクリーニングした。まず、現在市販されている 16 種類の TNFsf を、OVA と共に経鼻免疫し、全身面における免疫が誘導されるかどうかを、血清中の OVA 特異的 total IgG、IgG1、および IgG2a の誘導を指標に検討した（Fig. 1）。抗原特異的 total IgG の産生を測定した結果、TL1A は OVA 単独投与群と比較して、全身面において、有意な OVA 特異的 IgG 産生の増加がみられ、ポジティブコントロールとしての CT-B に匹敵する抗体産生能を有していた。また IgG のサブクラスである、IgG1 の産生を検討した結果からも、TNF-α、ならびに TL1A は有意に抗原特異的 IgG1 の産生を惹起していた。また、IgG2a の産生は、上昇傾向にはあるものの、有意な上昇は認められなかった。次に、粘膜面における免疫誘導を、腸管、膣および鼻粘膜組織における、OVA 特異的 IgA の産生を指標に検討した(Fig. 2)。その結果、いずれの粘膜面においても TL1A は抗原単独投与群と比較して、抗体産生能が有意に向上しており、特に鼻粘膜組織においては、タンパク量あたりに換算した CT-B（1 μg 投与群）と同等の活性を有している可能性が示唆された。更に、免疫マウスから回収した脾細胞を用いて各種 TNFsf の免疫誘導特性を、サイトカインアレイ(Fig. 3, 4)および ELISPOT アッセイ(Fig. 5)を用いて解析した。その結果、サイトカインアレイを用いた結果から、TL1A 投与群は、CT-B をアジュバントとして用いた群と比較し、IL-2、IL-4、IL-5、および GM-CSF 産生を有意に促進し、特に IL-4、IL-5 などの Th2 型サイトカイン産生誘導を有意に増強する傾向にあることが明らかとなった。一方で、ELISPOT アッセイの結果から、IFNγ 産生脾細胞数は、TL1A をアジュバントとして用いた群では、上昇しておらず、むしろ TRAIL、TRANCE、TWEAK 等の TNFsf の方が産生細胞数の上昇を惹起する可能性が示唆された。

**D. 考　察**

これまでTNFsfは強い免疫誘導能を有することが知られており、CD40L、LIGHT、OX40L などは、注射によるワクチンにおいて強いアジュバント能を有することが知られている。しかし、種々TNFsf を粘膜ワクチンアジュバントとして用い、その中から有効なTNFsfをスクリーニングした報告はこれまでにない。本研究では、現在市販されているTNFsf を粘膜ワクチンとして応用するため、16 種類の TNFsf の中から、有効な粘膜ワクチンアジュバントとして利用できる分子をスクリーニングした。その結果、TL1A が、粘膜ワクチンアジュバントとして、最も期待される分子の一つであることが示唆された。TL1A は、1997 年に同定され、T 細胞および B 細胞を除く、多くの細胞で発現していることが Northern Blot の結果から明らかになっている。TL1A は一方で、血管内皮細胞増殖抑制分子(VEGI)とも呼ばれ、血管の増殖を阻害する分子としても知られている。TL1A の受容体は、Death Receptor-3 (DR3)および、Decoy receptor-3 (DCR3)が知られており、これらの受容体は、血漿中にも可溶型で存在する以外にも、DR3 は、脾臓、胸腺、および末梢血リンパ球、DCR3 は、胎児の肺、脳、肝臓、および成人脾臓、腸管、肺にもそれぞれ発現することが知られている。現在、この TL1A が誘導する強い粘膜ワクチンアジュバント効果に関して、受容体の発現パターンとそのシグナル伝達の面から解析しているところである。今後は、前年度の TNF リジン欠損体の持つワクチンアジュバントとしての有用性が明らかになっていることから、この TL1A に関して、リジン欠損体を作製し、その有用性を検討していくことで、より有効性に優れた TNF スーパーファミリーを利用した粘膜ワクチンアジュバント開発に有効活用できるものと期待される。

## E. 結論

本研究では、現在市販されている 16 種類の TNFsf の中から、粘膜ワクチンアジュバントとして最も有効であることが示唆される TL1A を見出し、その優れた粘膜ワクチンアジュバント効果を確認した。可能であれば、来年度以降に、このリジン欠損 TL1A 変異体を作成し、N 末端部位特異的バイオコンジュゲーションすることで、より安全性・有効性に優れた粘膜ワクチンアジュバントの創製を試みる予定である。

## G. 研究発表

### ①論文発表


1. Abe Y., Yoshikawa T., **Kamada H.**, Shibata H., Nomura T., Minowa K., Kayamuro H., Katayama K., Miyoshi H., Mukai Y., Yoshioka Y., Nakagawa S., Tsunoda S., Tsutsumi Y. : Simple and highly sensitive assay system for TNFR2-mediated soluble- and transmembrane-TNF activity., J. Immunol. Methods., 335:71-8, 2008.
2. Imai S., Mukai Y., Takeda T., Abe Y., Nagano K., **Kamada H**., Nakagawa S., Tsunoda S., Tsutsumi Y. The effect of protein properties on display efficiency using the M13 phage display system. Pharmazie. 63(10):760-764, 2008.


### ②学会発表

国内

1. 渡辺　光, 吉岡靖雄, 森重智弘, **鎌田春彦**, 向洋平, 角田慎一, 堤　康央, 岡田直貴, 中川晋作. ファージ表面提示法を用いた活性増強型リンフォトキシンの創製とその特性評価. 第 8 回 日本蛋白質科学会年会, 2008 年 6 月, 東京.
2. 萱室裕之, 吉岡靖雄, 形山和史, **鎌田春彦**, 野村鉄也, 阿部康弘, 廣井隆親, 角田慎一, 堤　康央：TNFスーパーファミリーに着目した粘膜ワクチンアジュバント能の体系的評価., 第 56 回 日本ウイルス学会学術集会, 岡山, 2008 年 10 月.
3. **鎌田春彦**, 萱室裕之, 吉岡靖雄, 形山和史, 廣井隆親, 阿部康弘, 角田慎一, 堤　康央：活性増強型　TNF□構造変異体の粘膜ワクチンアジュバントへの応用., 第 22 回 日本エイズ学会学術集会, 大阪, 2008 年 11 月.
4. 萱室裕之, 吉岡靖雄, 阿部康弘, 形山和史, **鎌田春彦**, 野村鉄也, 廣井隆親, 角田慎一, 堤康央: 活性増強型TNF変異体の粘膜ワクチンアジュバ

ントへの応用., ファーマバイオフォーラム 2008, 東京, 2008 年 11 月.

5. 萱室裕之, 吉岡靖雄, 形山和史, **鎌田春彦**, 野村鉄也, 阿部康弘, 廣井隆親, 角田慎一, 堤 康央 : A bioactive mutant TNF (mTNF-K90R) elicited mucosal and systemic immunity against HIV-1 gp120 and influenza virus hemagglutinin., 第 38 回 日本免疫学会・学術集会, 京都, 2008 年 12 月.

海外

1. Kayamuro H., Yoshioka Y., Katayama K., **Kamada H.**, Nomura T., Abe Y., Hiroi T., Tsunoda S., Tsutsumi Y. MUTANT TNF ELICITS TH2-TYPE RESPONSES FOR ENHANCED MUCOSAL IMMUNITY. 7th Joint Conference of the Intenational Society for Interderon and Cytokine Research and International Cytokine Society. 12-16 October, 2008, Montréal/Québec, CANADA.
2. Yoshioka Y., Kayamuro H., Katayama K., **Kamada H.**, Abe Y., Hiroi T., Tsunoda S., Tsutsumi Y. IDENTIFICATION OF NEW CANDIDATES AS MUCOSAL VACCINE ADJUVANT IN TNF SUPERFAMILY CYTOKINES. FIMSA 2008. 17-20 October, 2008, Taipei, Taiwan.

**H. 知的財産権の出願・登録状況**

**①特許取得**

該当事項無し

**②実用新案登録**

該当事項無し

**③その他**

該当事項無し

**I. 研究協力者**

萱室裕之　大阪大学大学院薬学研究科　医薬基盤化学分野　博士後期課程 2 年

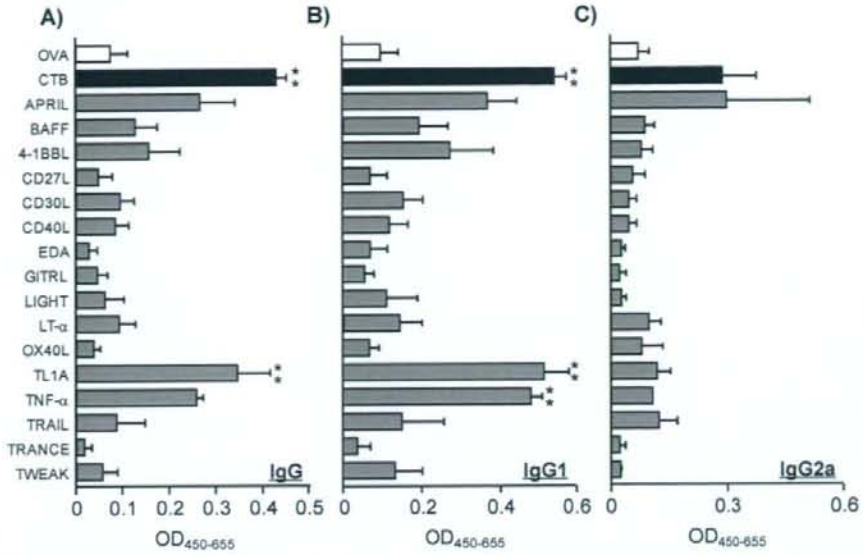


Figure 1. Serum OVA-specific IgG responses by nasal immunization with OVA plus TNF superfamily cytokines. BALB/c mice were intranasally immunized with OVA alone, OVA plus CTB, or OVA plus each TNF superfamily cytokine three times at weekly intervals. Serum was collected 7 days after last immunization and analyzed by ELISA for OVA-specific (A) total IgG, (B) IgG1 and (C) IgG2a responses at a 500 fold dilution of serum. Data are presented as means ± SEM (n = 5; ** $P < 0.01$ versus value for OVA alone treated group by ANOVA).

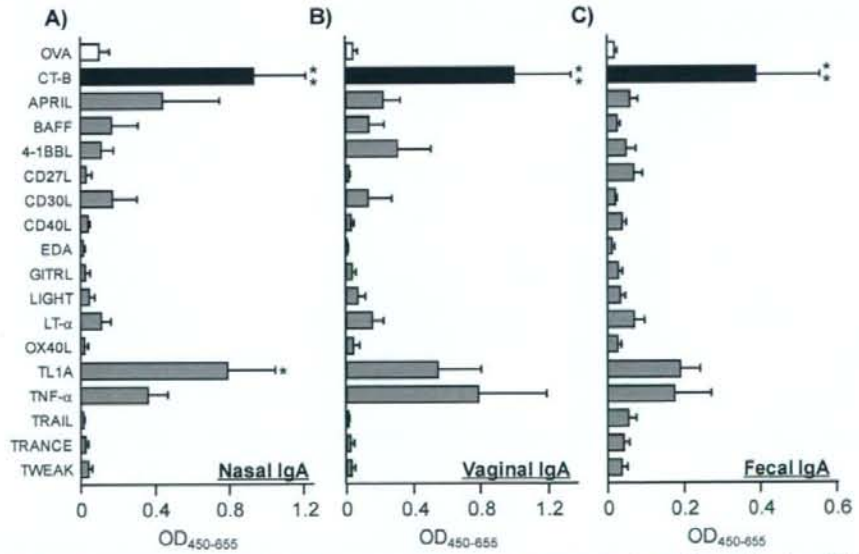


Figure 2. OVA-specific mucosal IgA responses by nasal immunization with OVA plus TNF superfamily cytokines. BALB/c mice were intranasally immunized with OVA alone, OVA plus CTB, or OVA plus each TNF superfamily cytokines once a week three times at weekly intervals. Mucosal secretions was collected seven days after last immunization and OVA-specific IgA responses in (A) nasal wash, (B) vaginal wash and (C) fecal extract were determined by ELISA, respectively. Data are presented as means ± SEM (n = 5; * $P < 0.05$, ** $P < 0.01$ versus value for OVA alone treated group by ANOVA).

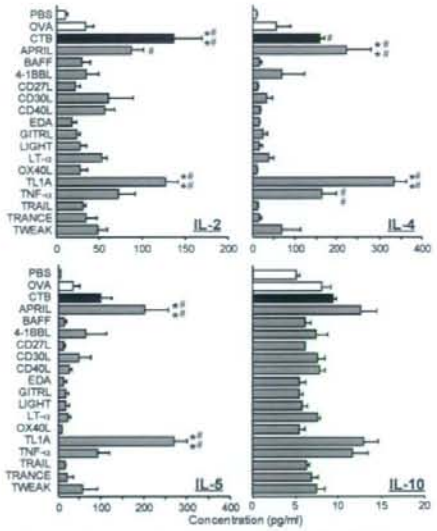


Figure 3. Cytokine responses induced by nasal immunization with OVA plus adjuvants. BALB/c mice were intranasally immunized with OVA alone, OVA plus CTB, OVA plus each TNF superfamily cytokine three times at weekly intervals. Seven days after last immunization, splenocytes from each group were cultured with 1 mg/ml OVA. Culture supernatants were harvested following 3 days of incubation, and OVA-specific IL-2, IL-4, IL-5 and IL-10 productions in culture supernatant were analyzed by using the Bio-Plex Multiplex Cytokine Assay. Data are presented as means ± SEM (n = 4; $^{\#}P < 0.05$, $^{\#\#}P < 0.01$ versus value for PBS treated group by ANOVA; ** $P < 0.01$ versus value for OVA alone treated group by ANOVA).

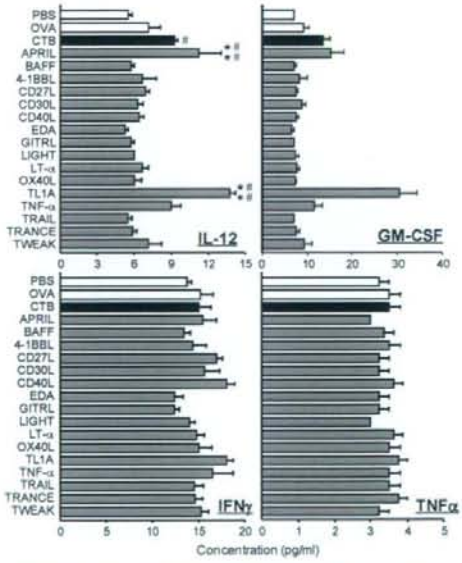


Figure 4. Cytokine responses induced by nasal immunization with OVA plus adjuvants. BALB/c mice were intranasally immunized with OVA alone, OVA plus CTB, OVA plus each TNF superfamily cytokine three times at weekly intervals. Seven days after last immunization, splenocytes from each group were cultured with 1 mg/ml OVA. Culture supernatants were harvested following 3 days of incubation, and OVA-specific (A) IL-4, (B) IL-5, (C) IFNγ and (D) TNF-α productions in culture supernatant were analyzed by using the Bio-Plex Multiplex Cytokine Assay. Data are presented as means ± SEM (n = 4; $^{\#}P < 0.05$, $^{\#\#}P < 0.01$ versus value for PBS treated group by ANOVA; ** $P < 0.01$ versus value for OVA alone treated group by ANOVA).

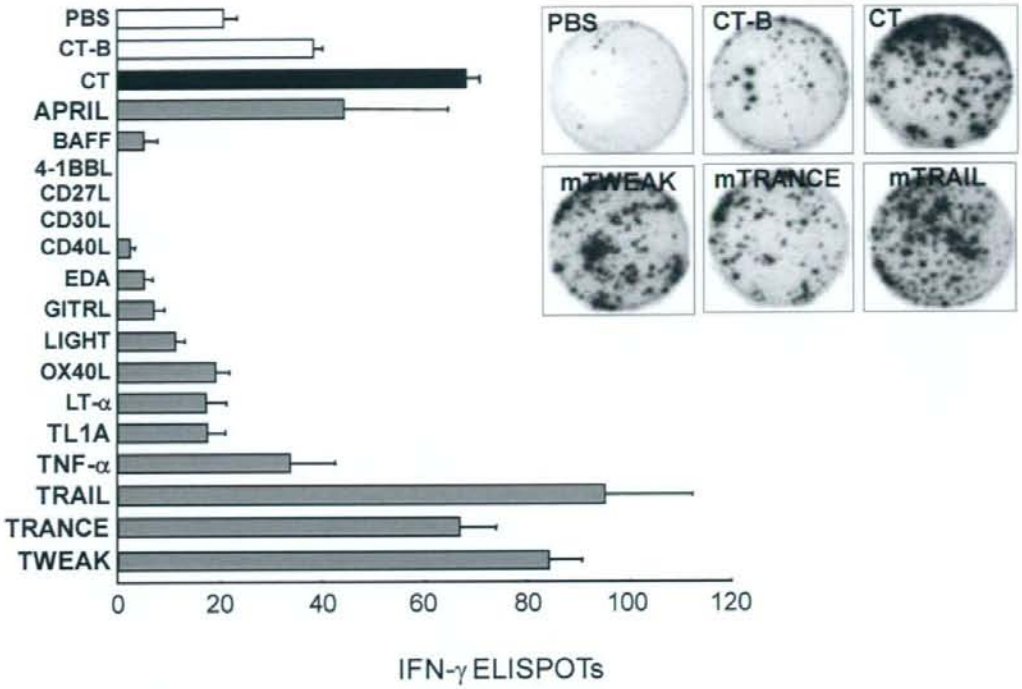


Figure 5. Analysis of OVA-specific cytokine-secreting cells in mice nasally immunized with OVA plus adjuvant. BALB/c mice were intranasally immunized with OVA alone, OVA plus 1 μg CTB, OVA plus 1 μg TNF super family members once a week for three consecutive weeks. One week after the last immunization, splenocytes from each group were cultured with 1 mg/ml OVA. The numbers of IFN-□-producing cells were examined by individual cytokine-specific ELISPOT assay. Data are presented as means ± SEM.

研究成果の刊行に関する一覧表

雑誌

| 発表者氏名 | 論文タイトル名 | 発表誌名 | 巻号 | ページ | 出版年 |
|---|---|---|---|---|---|
| Imai S., Mukai Y., Takeda T., Abe Y., Nagano K., Kamada H., Nakagawa S., Tsunoda S., Tsutsumi Y. | The effect of protein properties on display efficiency using the M13 phage display system. | Pharmazie | 63(10) | 760-764 | 2008 |
| Abe Y., Yoshikawa T., Kamada H., Shibata H., Nomura T., Minowa K., Kayamuro H., Katayama K., Miyoshi H., Mukai Y., Yoshioka Y., Nakagawa S., Tsunoda S., Tsutsumi Y. | Simple and highly sensitive assay system for TNFR2-mediated soluble- and transmembrane-TNF activity. | J. Immunol. Methods | 335(1-2) | 71-8 | 2008 |

Laboratory of Pharmaceutical Proteomics[1], National Institute of Biomedical Innovation (NIBIO), Graduate School of Pharmaceutical Sciences[2], Center of Advanced Medical Engineering and Informatics[3], Osaka University, Osaka, Japan

# Effect of protein properties on display efficiency using the M13 phage display system

S. Imai[1, 2], Y. Mukai[1, 2], T. Takeda[1], Y. Abe[1], K. Nagano[1, 2], H. Kamada[1, 3], S. Nakagawa[2], S. Tsunoda[1, 3], Y. Tsutsumi[1, 2, 3]

*Received May 15, 2008, accepted May 21, 2008*

*Shin-ichi Tsunoda, Ph.D., Laboratory of Pharmaceutical Proteomics, National Institute of Biomedical Innovation (NIBIO), 7-6-8 Saito-Asagi, Ibaraki, Osaka 567-0085, Japan*
*tsunoda@nibio.go.jp*

*Pharmazie 63: 760–764 (2008)* *doi: 10.1691/ph.2008.8132*

The M13 phage display system is a powerful technology for engineering proteins such as functional mutant proteins and peptides. In this system, it is necessary that the protein is displayed on the phage surface. Therefore, its application is often limited when a protein is poorly displayed. In this study, we attempted to understand the relationship between a protein's properties and its display efficiency using the well-known pIII and pVIII type phage display system. The display of positively charged SV40 NLS and HIV-1 Tat peptides on pIII was less efficient than that of the neutrally charged RGDS peptide. When different molecular weight proteins (1.5–58 kDa) were displayed on pIII and pVIII, their display efficiencies were directly influenced by their molecular weights. These results indicate the usefulness in predicting a desired protein's compatibility with protein and peptide engineering using the phage display system.

## 1. Introduction

Phage display systems have attracted much attention as the best technology to create functional mutant proteins and peptides ever since Smith et al. reported that random peptides could be displayed on the surface of filamentous M13 phage (Smith 1985). Many researchers have applied this system in attempts to create human antibodies and tissue-specific peptides (Schier et al. 1996; Maruta et al. 2003; Imai et al. 2006). Indeed, we have been successful in creating a useful mutant TNF to be used as a drug (Shibata et al. 2004; Yamamoto et al. 2003). Thus, the phage display system has a wide range of applications (Stich et al. 2003; Gourdine et al. 2005; Takashima et al. 2000).

Filamentous M13 phage has a circular single stranded DNA and takes the form of a long tube that consists of eleven kinds of proteins. This virus effectively proliferates upon infection of *E. coli* (Sidhu 2001; Bayer and Feigenson 1985; Kuhn 1987). In the phage display system, a fusion protein composed of target-molecule and coat protein is derived from a phagemid vector, and wild-type phage composition proteins (pI–pXI) are derived from a helper phage genome. These components can make phage libraries that display target-molecules by assembling within the periplasm of *E. coli*. The most useful characteristic of this system is that protein libraries can be displayed easily on the phage surface by inserting gene libraries within the phage genome. Target-molecules are obtained rapidly by the use of an *in vitro* affinity panning procedure that selects and amplifies specific phage clones (Smith 1985).

In the phage display system, target-molecules can be displayed on coat proteins (pIII, pVI, pVII, pVIII, pIX), though generally they are displayed on pIII or pVIII. Displaying 0–1 molecule per phage in the pIII type phage display system is suitable for isolating high-affinity molecules (Chasteen et al. 2006; Keresztessy et al. 2006). Alternatively, ten molecules can be displayed on a phage particle in the pVIII type phage display system to select low-affinity molecules (Verhaert et al. 1999; Kneissel et al. 1999; Lowman 1997).

As described, the phage display system is the most useful tool to create bioactive peptides and functional mutant proteins. However, because the efficiency of display is influenced by the properties of the target protein (molecular weight, electric charge, etc.), poor display often limits its application. Despite this problem, there is little research examining the relationship between display efficiency and a protein's properties. Thus, studies are warranted in order to apply the phage display system effectively. In this report, we prepared phages that displayed proteins of different molecular weights and electric charges to ascertain the relationship between display efficiency and protein properties.

## 2. Investigations, results and discussion

In this study we examined the relationship between protein properties (molecular weight, electric charge etc.) and the efficiency of display with pIII and pVIII coat proteins of the filamentous M13 phage display system (Fig. 1). To begin with, we prepared phages that displayed different electrically charged peptides on pIII (Fig. 2B) and evalu-

A)

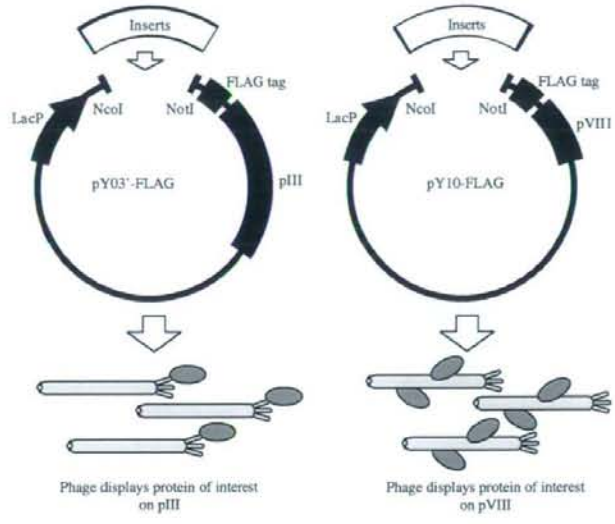


B)

| Inserts | Molecular weight (Da) | pI |
|---|---|---|
| RGDS peptide (RGDS) | 443 | 6.4 |
| SV40 NLS peptide (PKKKRKV) | 883 | 11.9 |
| HIV-Tat peptide (YGRKKRRQRRR) | 1,559 | 12.8 |
| LacZ-α | 11,000 | 5.2 |
| anti-KDR scFv | 25,000 | 5.0 |
| Importin-α | 58,000 | 5.1 |

Fig. 1:
Construction of phagemid vectors encoding different proteins or peptides.
A) Different inserts were cloned into pY03′-FLAG and pY10-FLAG phagemid vectors. Phage particles displaying proteins fused to pIII and pVIII were prepared from pY03′-FLAG and pY10-FLAG, respectively. B) Different inserts and their molecular weights

A)

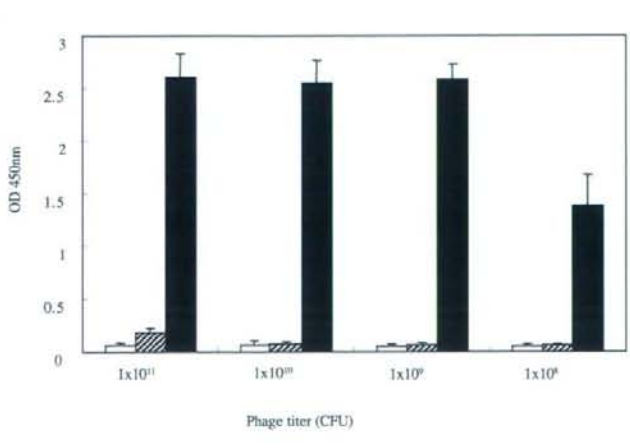


B)

| | sequence | M.W. (Da) | pI |
|---|---|---|---|
| □ Tat peptide | YGRKKRRQRRR | 1,559 | 12.8 |
| ▩ SV40 NLS | PKKKRKV | 883 | 11.9 |
| ■ RGDS peptide | RGDS | 433 | 6.4 |

Fig. 2:
Influence of the efficiency of peptide-display by the ionic charge of peptides.
The efficiency of peptide-display on pIII was assessed by phage ELISA. Displayed peptides were fused to FLAG-tag – pIII on the phage particle and captured by immobilized anti-FLAG antibody. After washing, the number of captured phage was assessed by anti-M13 HRP conjugate. Two positively charged peptides (Tat peptide; □ and SV40 NLS; ▩) and a neutral peptide (RGDS; ■) were used in this experiment (n = 3). Each data value represents the mean ± S.D. B) Sequences of displayed peptides and their pIs. Cationic amino acids are underlined. All pI values were calculated by Expasy Compute pI/Mw tool (http://au.expasy.org)

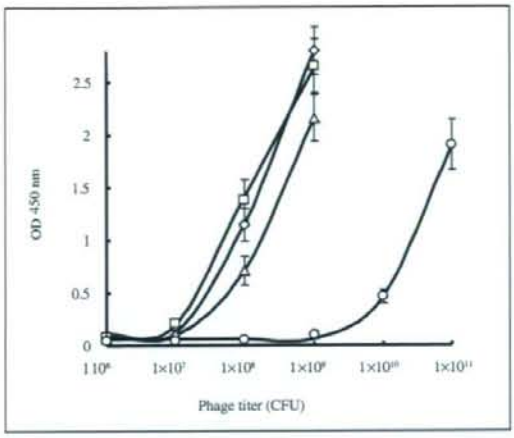


Fig. 3: Comparison of the efficiency of protein-display using pIII type phage display.
The efficiency of protein-display on pIII was assessed by phage ELISA. Proteins with different molecular weights (approximately 400–58,000 Da) were displayed on phage particle as pIII fusion proteins. This experiment was performed using the same method as Fig. 2 (n = 3). Each data value represents the mean ± S.D. □, RGDS-pIII phage; ◇, LacZ-pIII phage; △, scFv-pIII phage; ○, Importin-α-pIII phage

ated the relationship between electric charge and display efficiency using FLAG tagged ELISA (Fig. 2A). The display of positively charged SV40 NLS and HIV-1 Tat peptides were less efficient than that of the neutrally charged RGDS peptide. Generally, positively charged peptides are easy to adsorb onto various surfaces (Gaillard et al. 1999), and they repulse each other. Therefore, positively charged peptides may interfere with phage assembly in the periplasm.

Second, we examined the relationship between molecular weight and display efficiency again using FLAG tagged ELISA (Fig. 3). Because the display of positively charged sample was less efficient (Fig. 2), we used the neutrally charged proteins (pI 5.0–6.4) (MW 1.5–58 kDa) displayed on pIII to examine the influence of molecular weight on display. Phage displaying the low molecular weight RGDS peptide bound to anti-FLAG antibody at a concentration of $10^6$–$10^9$ CFU. The higher molecular weight importin-α (58 kDa) displayed on the phage surface could not bind at the same concentration, needing $10^9$–$10^{11}$ CFU. In general, the amount of phage prepared by following the standard protocol was approximately $10^{12}$–$10^{13}$ CFU (Imai 2006). To create functional mutants using a phage library, it is desirable to use an amount of phage in excess (more than 100-fold) of the phage library (approximately $10^6$–$10^9$ CFU). When proteins display on the phage surface efficiently, the experiment can proceed without bias. However, our result suggests that a phage library displaying high molecular weight proteins may be of low quality simply because the levels of the desired proteins are not sufficiently expressed for screening. This introduces a selection bias for those proteins that can be expressed at the proper level.

To examine the efficiency of pIII-display in greater detail, we quantified the number of molecules displayed on the phage surface by electrophoresis analysis using CsCl purified phage (Fig. 4). These results (Fig. 3, 4) demonstrate that the efficiency of RGDS peptide-display on pIII was the best (approximately 2 molecules/phage). The display efficiency decreased as the molecular weight of the target protein increased. Because the titer of all phages prepared in this experiment was determined, we suggested that the display of different molecular weight proteins did not affect the efficiency of phage-preparation (data not shown). Additionally, the proteins used in this experiment (RGDS, LacZ, scFv and importin-α) were expressed efficiently in *E. coli*. Therefore, we suggest that the efficiency with which a protein is displayed on pIII is directly related to its molecular weight.

Finally, we examined the efficiency of pVIII-display by Western blot and confirmed that it also decreased as the molecular weight increased (Fig. 5). Interestingly, this result shows that scFv (25 kDa) could be displayed on pVIII efficiently. Because the pVIII phage display system is generally believed to be limited in its application precisely by the molecular weight of displayed protein, many used it only for display of peptide libraries (Verhaert et al. 1999; Kneissel et al. 1999; Lowman 1997; Gaillard et al. 1999). However, our result suggests that the pVIII system could be applied to larger molecules. This could provide useful

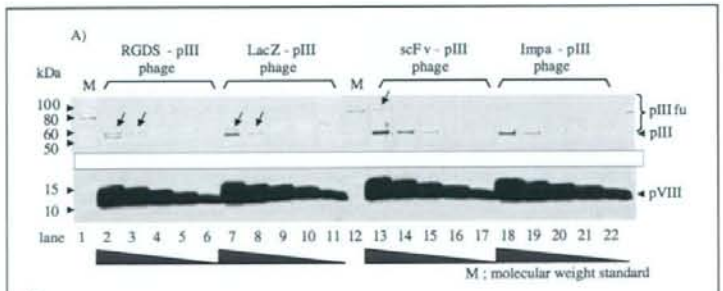


B)

| | RGDS-pIII | LacZ-pIII | scFv-pIII | Impα-pIII |
|---|---|---|---|---|
| M.W. of displayed protein (kDa) | 1.5 | 11 | 25 | 58 |
| M.W. of pIII fusion protein (kDa) | 52.5 | 62 | 76 | 109 |
| Number of displayed proteins/phage | 2.7 | 1.0 | 0.12 | N.D. |

N.D.; Not Detectable

Fig. 4:
Calculated quantity of pIII displayed proteins using Sypro® Ruby staining.
A) The efficiency of display on pIII was quantified using CsCl purifed phages. RGDS-pIII (lanes 2–6), LacZ-pIII (lanes 7–11), scFv-pIII (lanes 13–17) and Impα-pIII phage (lanes 18–22) were used in this experiment. Molecular weight standard was loaded in lanes 1 and 12. Starting from the left, $1 \times 10^{13}$ vp, $3.3 \times 10^{12}$ vp, $1.1 \times 10^{12}$ vp, $3.7 \times 10^{11}$ vp and $1.2 \times 10^{11}$ vp were loaded. B) The number of displayed proteins per one phage particle was calculated by fluorescence image analysis. Fluorescence intensity was quantified by Typhoon image analyzer

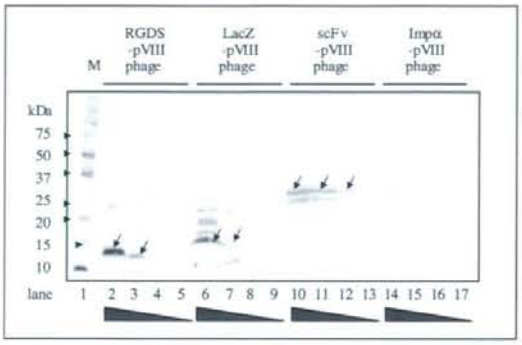


Fig. 5: Comparison of the efficiency of pVIII display protein on phage particles.
The efficiency of display on pVIII was assessed by anti-FLAG western blot. PEG-purified RGDS-pVIII (lanes 2–5), LacZ-pVIII (lanes 6–9), scFv-pVIII (lanes 10–13) and Impα-pVIII phage (lanes 14–17) were used in this experiment. Molecular weight standard was loaded in lane 1. Starting from the left, $1.5 \times 10^{11}$ cfu, $5 \times 10^{10}$ cfu, $1.7 \times 10^{10}$ cfu and $5.5 \times 10^{9}$ cfu were loaded

additional information by expanding the application of phage display systems to create various mutant proteins.
In this study, different kinds of sample peptides (SV40 NLS, HIV-1 Tat, RGDS) and proteins (RGDS, LacZ, scFv, importin-α) that could be readily expressed in *E. coli* were used as model molecules. The display of positively charged SV40 NLS and HIV-1 Tat peptides on pIII was less efficient than that of the neutrally charged RGDS peptide. When different molecular weight proteins (1.5–58 kDa) were displayed on pIII and pVIII, their display efficiencies were directly related to their molecular weights.
When comparing the efficiency of display between the four model proteins, additional factors (i.e. refolding efficiency, etc.) may account for the differences. These results show at least that the electric charge affected the efficiency of phage display and that high molecular weight proteins could not be displayed on the phage surface successfully. Recently, it was reported that improving the phagemid vector provided better efficiency of protein refolding in *E. coli* and enhanced protein display on the phage surface (Guo et al. 2003). Consequently many hope that the display efficiency of various molecules could be improved using this methodology. However, while this method improves the quality of fusion protein expression, it does not take into account the efficiency of protein assembly for the construction of phage particles. Therefore, it is still important to be able to predict the molecules that will be compatible for protein and peptide engineering using phage display by understanding the properties of this system as they were described in this report.

## 3. Experimental

### *3.1. Phagemid vectors and inserts*

The pY03′-FLAG phagemid vector was modified from pCANTAB-5E (GE Healthcare Ltd.). To create this vector, the E-tag from the original vector was changed to a FLAG tag (DYKDDDDK). The pY10-FLAG phagemid vector was constructed by replacing the pIII gene in pY03′-FLAG with the pVIII gene. Genes encoding peptides (RGDS, HIV-Tat, SV40 NLS) were synthesized by Operon Biotechnologies Inc., USA. The lacZ-α gene had already been cloned into pY03′-FLAG and pY10-FLAG. The anti-KDR scFv gene was isolated from an optimized non-immune phage antibody library previously described (Imai et al. 2006). The human importin-α gene was amplified from a human bone marrow cDNA library (TAKARA Bio. Inc.). These inserts were digested and cloned into each phagemid vector.

### *3.2. Phage preparation*

Phage was prepared by following a standard protocol. Briefly, phage particles were prepared from *Escherichia coli* (TG1 strain, Stratagene corporation) by co-infection with M13KO7 helper phage (Invitrogen Corporation). Amplified phage in culture media was roughly purified by PEG precipitation. Part of the purified phage was added to the TG1 bacteria, and the phage titer (cfu) was calculated by counting infected TG1 colonies. If necessary, additional purification using a CsCl gradient was performed as described below.

### *3.3. Phage ELISA*

Immunoplates (Nalge Nunc International) were immobilized with anti-FLAG M2 antibody (Sigma-Aldrich Corporation) diluted to 5 μg/ml in bicarbonate buffer (Sigma-Aldrich Corporation). Plates were blocked with 2% block ace (Nakarai Tesque Inc.) for 2 h at 37 °C. Phage solution (PEG-purified) in 0.4% block ace was serially diluted and applied to the wells. After a 1 h incubation at room temperature, the binding phage was detected by anti-M13 HRP conjugate (GE Healthcare Ltd.).

### *3.4. Purification of phage particles under CsCl gradient*

Amplified phage was purified by PEG precipitation. Phage pellets were resuspended in TBS buffer. CsCl powder (IWAI chemicals company) and additional TBS buffer were added to the phage solution up to 31%. After CsCl gradient ultracentrifugation at 400,000 × g at 5 °C for 20 h, the concentrated phage band was isolated. TBS (five volumes) was added to the purified phage and centrifuged again at 400,000 × g at 5 °C for 4 h to remove the CsCl. The obtained phage was resuspended in TBS and used for experiments.

### *3.5. Sypro Ruby staining*

After purifying the phage under a CsCl gradient, the number of phage particles (vp/ml) was estimated from its absorbance according to the standard protocol. Serially diluted phage samples were resolved by SDS – poly acrylamide electrophoresis (SDS-PAGE). Gels were incubated in SYPRO® Ruby protein gel stain reagent (Pearce Biotechnology, Inc., USA) overnight at room temperature. After washing with wash buffer (10% methanol and 7% acetic acid) for 30 min, fluorescence was detected using the Typhoon Variable Image Analyzer (GE Healthcare Ltd.). The number of surface-displayed proteins was calculated from fluorescence intensity using ImageQuant TL software (GE Healthcare Ltd.) assuming that one phage particle contained five pIII coat proteins on its surface.

### *3.6. Anti-FLAG western blotting*

SDS-PAGE was performed using serially diluted phage purified by PEG precipitation. Phage protein in the gel was transferred to PVDF membrane (GE Healthcare Ltd.) using the Hoefer TE 70 semi dry transfer unit (GE Healthcare Ltd.). Membranes were blocked in 4% block ace for 1 h. FLAG-tagged pVIII fusion protein was detected with anti-FLAG M2 antibody (Sigma-Aldrich Corporation) and anti-mouse IgG HRP conjugate (Sigma-Aldrich Corporation). After detection by ECL plus reagent (GE Healthcare Ltd.), its luminescence was quantitated using the LAS-3000 Lumi Imager (Fujifilm Corporation).

Acknowledgements: This study was supported in part by Grants-in-Aid for Scientific Research (No. 20015052) from the Ministry of Education, Culture, Sports, Science and Technology of Japan, by Health and Labor Sciences Research Grant from the Ministry of Health, Labor and Welfare of Japan, and in part by Research Fellowships for Young Scientists (No. 3608) from Japan Society for the Promotion of Science.

**References**

Bayer R, Feigenson GW (1985) Reconstitution of M13 bacteriophage coat protein. A new strategy to analyze configuration of the protein in the membrane. Biochim Biophys Acta 815: 369–379.
Chasteen L, Ayriss J, Pavlik P, Bradbury AR (2006) Eliminating helper phage from phage display. Nucleic Acids Res 34: e145.
Gaillard C, Flavin M, Woisard A, Strauss F (1999) Association of double-stranded DNA fragments into multistranded DNA structures. Biopolymers 50: 679–689.
Gourdine JP, Greenwell P, Smith-Ravin E (2005) Application of recombinant phage display antibody system in study of Codakia orbicularis gill proteins. Appl Biochem Biotechnol 125: 41–52.
Guo JQ, You SY, Li L, Zhang YZ, Huang JN, Zhang CY (2003) Construction and high-level expression of a single-chain Fv antibody fragment specific for acidic isoferritin in Escherichia coli. J Biotechnol 102: 177–189.
Imai S, Mukai Y, Nagano K, Shibata H, Sugita T, Abe Y, Nomura T, Tsutsumi Y, Kamada H, Nakagawa S, Tsunoda S (2006) Quality enhancement of the non-immune phage scFv library to isolate effective antibodies. Biol Pharm Bull 29: 1325–1330.

Keresztessy Z, Csosz E, Harsfalvi J, Csomos K, Gray J, Lightowlers RN, Lakey JH, Balajthy Z, Fesus L (2006) Phage display selection of efficient glutamine-donor substrate peptides for transglutaminase 2. Protein Sci 15: 2466–2480.

Kneissel S, Queitsch I, Petersen G, Behrsing O, Micheel B, Dubel S (1999) Epitope structures recognised by antibodies against the major coat protein (g8p) of filamentous bacteriophage fd (Inoviridae). J Mol Biol 288: 21–28.

Kuhn A (1987) Bacteriophage M13 procoat protein inserts into the plasma membrane as a loop structure. Science 238: 1413–1415.

Lowman HB (1997) Bacteriophage display and discovery of peptide leads for drug development. Annu Rev Biophys Biomol Struct 26: 401–424.

Maruta F, Parker AL, Fisher KD, Murray PG, Kerr DJ, Seymour LW (2003) Use of a phage display library to identify oligopeptides binding to the lumenal surface of polarized endothelium by ex vivo perfusion of human umbilical veins. J Drug Target 11: 53–59.

Schier R, Bye J, Apell G., McCall A, Adams GP, Malmqvist M, Weiner LM, Marks JD (1996) Isolation of high-affinity monomeric human anti-c-erbB-2 single chain Fv using affinity-driven selection. J Mol Biol 255: 28–43.

Shibata H, Yoshioka Y, Ikemizu S, Kobayashi K., Yamamoto Y, Mukai Y, Okamoto T, Taniai M, Kawamura M, Abe Y, Nakagawa S, Hayakawa T, Nagata S, Yamagata Y, Mayumi T, Kamada H, Tsutsumi Y (2004) Functionalization of tumor necrosis factor-alpha using phage display technique and PEGylation improves its antitumor therapeutic window. Clin Cancer Res 10: 8293–8300.

Sidhu SS (2001) Engineering M13 for phage display. Biomol Eng 18: 57–63.

Smith GP (1985) Filamentous fusion phage: novel expression vectors that display cloned antigens on the virion surface. Science 228: 1315–1317.

Stich N, Van Steen G, Schalkhammer T (2003) Design and peptide-based validation of phage display antibodies for proteomic biochips. Comb Chem High Throughput Screen 6: 67–78.

Takashima A, Mummert M, Kitajima T, Matsue H (2000) New technologies to prevent and treat contact hypersensitivity responses. Ann N Y Acad Sci 919: 205–213.

Verhaert RM, Van Duin J, Quax WJ (1999) Processing and functional display of the 86 kDa heterodimeric penicillin G acylase on the surface of phage fd. Biochem J 342: 415–422.

Yamamoto Y, Tsutsumi Y, Yoshioka Y, Nishibata T, Kobayashi K., Okamoto T, Mukai Y, Shimizu T, Nakagawa S, Nagata S, Mayumi T (2003) Site-specific PEGylation of a lysine-deficient TNF-alpha with full bioactivity. Nat Biotechnol 21: 546–552.

Journal of Immunological Methods 335 (2008) 71–78

Contents lists available at ScienceDirect

Journal of Immunological Methods

journal homepage: www.elsevier.com/locate/jim

Research paper

# Simple and highly sensitive assay system for TNFR2-mediated soluble- and transmembrane-TNF activity

Yasuhiro Abe [a,b], Tomoaki Yoshikawa [a,c], Haruhiko Kamada [a,d], Hiroko Shibata [a,e], Tetsuya Nomura [a,b], Kyoko Minowa [a,f], Hiroyuki Kayamuro [a,b], Kazufumi Katayama [g], Hiroyuki Miyoshi [h], Yohei Mukai [a,b], Yasuo Yoshioka [a,c], Shinsaku Nakagawa [b], Shin-ichi Tsunoda [a,d,*], Yasuo Tsutsumi [a,b,d]

[a] Laboratory of Pharmaceutical Proteomics, National Institute of Biomedical Innovation, 7-6-8 Saito-Asagi, Ibaraki, Osaka 567-0085, Japan
[b] Graduate School of Pharmaceutical Sciences, Osaka University, 1-6 Yamadaoka, Suita, Osaka 565-0871, Japan
[c] The Center for Advanced Research and Education in Drug Discovery and Development, Osaka University, 1-6 Yamadaoka, Suita, Osaka 565-0871, Japan
[d] The Center for Advanced Medical Engineering and Informatics, Osaka University, 1-6 Yamadaoka, Suita, Osaka 565-0871, Japan
[e] Division of Drugs, National Institute of Health Science, 1-18-1 Kamiyoga, Setagaya-ku, Tokyo 158-8501, Japan
[f] Graduate School of Pharmaceutical Sciences, Kyoto Pharmaceutical University, Misasagi-Nakauchicho 5, Yamashina-ku, Kyoto 607-8414, Japan
[g] Allergy & Immunology Project, Tokyo Metropolitan Institute of Medical Science, 3-18-22, Honkomagome, Bunkyo-ku, Tokyo 113-8613, Japan
[h] Subteam for Manipulation of Cell Fate, BioResource Center, RIKEN, 3-1-1 Koyadai, Tsukuba, Ibaraki 305-0074, Japan

ARTICLE INFO

*Article history:*
Received 25 December 2007
Received in revised form 28 February 2008
Accepted 28 February 2008
Available online 26 March 2008

*Keywords:*
TNF
TNFR2
Fas
Chimeric receptor
Bioassay

ABSTRACT

Drugs that target tumor necrosis factor-α (TNF) are particularly important in the treatment of severe inflammatory progression in rheumatoid arthritis, Crohn's disease and psoriasis. Despite the central role of the TNF/TNF receptor (TNFR) in various disease states, there is a paucity of information concerning TNFR2 signaling. In this study, we have developed a simple and highly sensitive cell-death based assay system for analyzing TNFR2-mediated bioactivity that can be used to screen for TNFR2-selective drugs. Using a lentiviral vector, a chimeric receptor was engineered from the extracellular and transmembrane domain of human TNFR2 and the intracellular domain of mouse Fas and the recombinant protein was then expressed in TNFR1$^{-/-}$ R2$^{-/-}$ mouse preadipocytes. Our results demonstrate that this chimeric receptor is capable of inducing apoptosis by transmembrane- as well as soluble-TNF stimuli. Moreover, we found that our bioassay based on cell death phenotype had an approximately 80-fold higher sensitivity over existing bioassays. We believe our assay system will be an invaluable research tool for studying TNFR2 and for screening TNFR2-targeted drugs.



## 1. Introduction

Tumor necrosis factor-α (TNF) is a pleiotropic cytokine that regulates various biological processes such as host defense, inflammation, autoimmunity, apoptosis and tumor cell death through the TNF-receptor 1 (TNFR1) and receptor 2 (TNFR2) (Wajant et al., 2003). TNF/TNFR interaction is considered to be an attractive target for the treatment of refractory diseases, including autoimmune disease and malignant tumors (Aggarwal, 2003; Szlosarek and Balkwill, 2003). In rheumatoid arthritis, for example, biological anti-TNF agents, such as Infliximab and Adalimumab, rapidly reduce signs and symptoms of joint inflammation (Feldmann and Maini, 2003). However, anti-TNF drugs used to treat inflammatory disorders have been reported to increase the risk of infection, in accordance with animal studies (Brown et al., 2002; Nathan et al., 2006).

* Corresponding author. Laboratory of Pharmaceutical Proteomics, National Institute of Biomedical Innovation, 7-6-8 Saito-Asagi, Ibaraki, Osaka 567-0085, Japan. Tel.: +81 72 641 9811x2327; fax: +81 72 641 9817.
*E-mail address:* tsunoda@nibio.go.jp (S. Tsunoda).

0022-1759/$ – see front matter © 2008 Elsevier B.V. All rights reserved.
doi:10.1016/j.jim.2008.02.019

A thorough understanding of the biology of the TNF/TNFR system is a prerequisite to the safe and effective development of anti-TNF therapeutics. In particular, several factors and mechanisms hypothesized to be involved in the side effects elicited by anti-TNF drugs need to be tested (Curtis et al., 2007; Jacobs et al., 2007; Schneeweiss et al., 2007). These include the differential power of the drugs to neutralize TNF bioavailability and the differential inhibition of TNF signaling events. Despite extensive studies on the molecular biology of TNF/TNFR1 signaling (Micheau and Tschopp, 2003) the functions of TNFR2 are poorly understood. There is an increasing need for a comprehensive understanding of TNF/TNFR2 biology, particularly in terms of the development of TNFR-selective drugs.

In this context, we have used a novel phage-display based screening system (Yamamoto et al., 2003; Shibata et al., 2004, 2008) to develop structural mutants of TNF to help clarify the biology of TNF/TNFR2 interactions. These TNF variants, which exert TNFR2-mediated agonistic or antagonistic activity, might be extremely valuable for elucidating structure-activity relationships between TNF and TNFR2. So far, in order to evaluate the bioactivity of TNF through TNFR2, many researchers have used the TNFR2 over-expressing cell lines (Heller et al., 1992; Weiss et al., 1998), such as rat/mouse T hybridomas transfected with human TNFR2 (PC60-hR2) (Vandenabeele et al., 1992). The PC60-hR2 assay is based on granulocyte macrophage colony-stimulating factor (GM-CSF) secretion mediated by TNF/TNFR2 stimuli. The GM-CSF secretion level is quantified by proliferation of GM-CSF-dependent cell lines or by ELISA. However, this two-step assay system is complicated and the screening process is highly laborious. Thus, there are increasing demands for the development of a simple, highly sensitive screening system that is TNFR2-selective.

In the present study, we developed a simple but highly sensitive cell death-based assay system for evaluating TNFR2-mediated activity. We constructed a lentiviral vector expressing a chimeric receptor derived from the extracellular (EC) and transmembrane (TM) domain of human TNFR2 (hTNFR2) and the intracellular (IC) domain of mouse Fas (mFas). Additionally, to eliminate the influence of the endogenous TNFR1, the chimeric receptor was expressed on TNFR1$^{-/-}$R2$^{-/-}$ preadipocytes (Xu et al., 1999). We found that hTNFR2/mFas-expressing preadipocyte (hTNFR2/mFas-PA) showed about 80-times higher sensitivity after treatment with soluble-TNF and over the conventional method. Furthermore, hTNFR2/mFas-PA could detect not only transmembrane TNF- (tmTNF) but also soluble TNF-activity. The technology described herein will be highly useful both as an assay system for various TNF variants *via* TNFR2 and also as a cell-based drug discovery system for TNFR2 agonists/antagonists.

## 2. Materials and methods

### 2.1. Cell culture

TNFR1$^{-/-}$R2$^{-/-}$, TNFR1$^{-/-}$, and wild-type (wt) preadipocytes established from day 16–17 mouse embryos were generously provided by Dr. Hotamisligil (Harvard School of Public Health, Boston MA). Preadipocytes, 293T cells and HeLaP4 cells were cultured in Dulbecco's modified Eagle's medium (DMEM; Sigma-Aldrich, Inc., Tokyo, Japan) with 10% bovine fetal serum (FBS) and 1% antibiotic cocktail (penicillin 10,000 u/ml, streptomycin 10 mg/ml, and amphotericin B 25 μg/ml; Nacalai Tesque, Kyoto, Japan). The rat/mouse T hybridomas PC60-hR2 cells (hTNFR2 transfected PC60 cells) were generously provided by Dr. Vandenabeele (University of Gent, Belgium) and cultured in RPMI 1640 (Sigma-Aldrich, Inc.) with 10% FBS, 1 mM sodium pyrubate, $5\times10^{-5}$ M 2-ME, 3 μg/ml puromycin (Wako Pure Chemical Industries, Osaka, Japan), and 1% antibiotic cocktail. TNFR1$^{-/-}$R2$^{-/-}$ mouse macrophages were generously provided by Dr. Aggarwal (University of Texas MD Anderson Cancer Center, Houston, TX), and cultured in RPMI 1640 with 10% FBS and 1% antibiotic cocktail.

### 2.2. Construction of self-inactivating (SIN) lentiviral vector

Vectors were constructed using standard cloning procedures. A DNA fragment encoding the EC and TM parts of hTNFR2 was amplified by polymerase chain reaction (PCR) from human peripheral blood lymphocyte cDNA with the following primer pairs: forward primer (5′-GAT TAC GCC AAG CTT GTC GAC CAC CAT GGC GCC CGT CGC CGT CTG GGC CGC GCT GGC CGT CGG ACT GGA G-3′) containing a SalI site at the 5′-end and a reverse primer (5′-CAC CTT GGC TTC TCT CTG CTT TCG AAG GGG CTT CTT TTT CAC CTG GGT CA-3′) containing a Csp45I site. The resulting amplified fragment was subcloned into pCR-Blunt II-TOPO (Invitrogen Corp., Carlsbad, CA) to generate pCR-Blunt-hTNFR2. A fragment encoding the IC domain of mFas was amplified by PCR from mouse spleen cDNA with the following primer pair: forward primer (5′-AAT TCC ACT TGT ATT TAT ACT TCG AAA GTA CCG GAA AAG A-3′) containing a Csp45I site and a reverse primer (5′-GTC ATC CTT GTA GTC TGC GGC CGC TCA CTC CAG ACA TTG TCC TTC ATT TTC ATT TCC A-3′) containing a NotI site at the 5′-end. The mFas DNA fragment was subcloned into pCR-Blunt-hTNFR2 between the Csp45I and NotI sites to combine the EC and TM domains of hTNFR2 to the IC domains of mFas, generating pCR-Blunt-hTNFR2/mFas (Fig. 1A). Then the hTNFR2/mFas DNA fragment was cloned between the XhoI and NotI sites of SIN lentiviral vector construct, which contains the blasticidin (Bsd) resistance gene, generating CSII-CMV-hTNFR2/mFas-IRES2-Bsd (Fig. 1B). For construct tmTNF, a DNA fragment encoding non-cleavable human tmTNF h(tmTNFΔ1-12), generated by deleting amino acids 1–12 in the N-terminal part of hTNF, was amplified by PCR from hTNF cDNA with following primer pair: forward primer (5′-AGT GAT CGG CCC CCA GAG GGA AGC TTA GAT CTC TCT CTA ATC AGC CCT CTG GCC CAG GCA GTA GCC CAT GTT GTA GCA AAC CCT CAA G-3′) and reverse primer (5′-GGT TGG ATG TTC GTC CTC CGC GGC CGC CTA ACT AGT TCA CAG GGC AAT GAT CCC AAA GTA GAC CTG-3′) and cloned into the pY03′ vector. Then tmTNFΔ1–12 DNA fragment was cloned between the SalI and XhoI sites of the SIN vector construct, generating CSII-EF-tmTNF-IRES-GFP.

### 2.3. Preparation of lentiviral vectors

The method used to prepare the lentiviral vector has been described previously (Miyoshi et al., 1999; Katayama et al.,

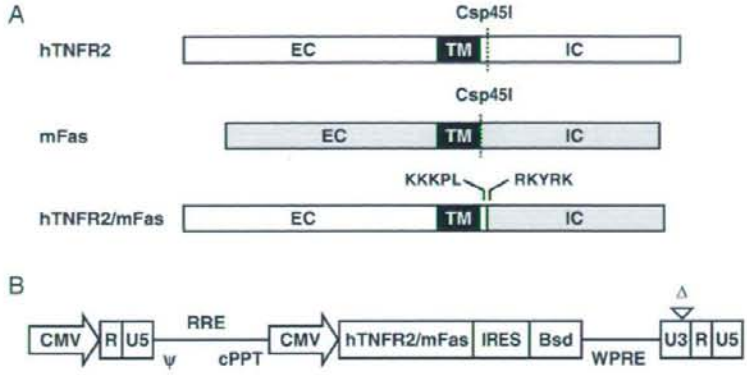


**Fig. 1.** Construction of hTNFR2/mFas chimeric receptor gene and vector. (A) The cDNA structures of hTNFR2, mFas and fusion genes (hTNFR2/mFas) are shown. EC: extracellular domain, TM: transmembrane domain, IC: Intracellular domain. (B) Schematic representation of self-inactivating (SIN) LV plasmid (CSII-CMV-hTNFR2/mFas-IRES-Bsd). CMV, cytomegalovirus promoter; ψ: packaging signal; RRE, rev responsive element; cPPT, central polypurine tract; IRES, Encephalomyocarditis virus internal ribosomal entry site; Bsd, Blasticidin; WPRE, woodchuck hepatitis virus posttranscriptional regulatory element. Δ: deleting 133 bp in the U3 region of the 3′ long terminal repeat.

2004). In brief, 293T cells were transfected by the calcium phosphate method with three plasmids: packaging construct (pCAG-HIVgp), VSV-G and Rev expressing construct (pCMV-VSV-G-RSV-Rev) and SIN vector construct (CSII-CMV-TNFR2/Fas-IRES2-Bsd or CSII-EF-tmTNF-IRES-GFP). Two days after transfection, the conditioned medium was collected and the virus was concentrated by ultracentrifugation at 50,000 × *g* for 2 h at 20 °C. The pelleted virus was resuspended in Hanks' balanced salt solution (GIBCO BRL, Paisley, UK). Vector titers were determined by measuring the infectivity of HeLaP4 cells with serial dilutions of vector stocks using flow cytometric analysis (FCM) for hTNFR2/mFas- or GFP-positive cells.

### 2.4. Preparation of hTNFR2/mFas- or tmTNF-expressing cell culture

To prepare the hTNFR2/mFas- or tmTNF-expressing cell culture, $TNFR1^{-/-}R2^{-/-}$ preadipocytes or $TNFR1^{-/-}R2^{-/-}$ macrophages were infected with each lentiviral vector at a multiplicity of infection (MOI) of 100. Stable hTNFR2/mFas-transfectants were selected for growth in culture medium containing 8 μg/ml Bsd (Invitrogen Corp.) for 1 week. Expression of hTNFR2/mFas chimeric receptor on Bsd-resistant cells was detected by staining with biotinylated anti-hTNFR2 antibody (BD Biosciences, Franklin Lakes, NJ) at 0.5 μg/$5 \times 10^5$ cells for 30 min at 4 °C. Subsequently, the cells were washed and stained with streptavidin-PE conjugate (BD Biosciences). The cell suspension was centrifuged at 800 × *g*, washed with PBS, centrifuged again, and then re-suspended in 500 μl of 0.4% paraformaldehyde. Fluorescence was analyzed on a FACS Vantage flow cytometer, and data were analyzed using CellQuest software (both BD Biosciences). The hTNFR2/mFas-positive cell cultures were used in subsequent experiments as hTNFR2/mFas-PA cells. For preparation of tmTNF-expressing $TNFR1^{-/-}R2^{-/-}$ macrophages (tmTNF-Mφ), IRES-driven GFP positive cells were sorted by FACSAria (BD Biosciences).

### 2.5. Cytotoxicity assays

Cells were seeded on 96-well micro titer plates at a density of $1.5 \times 10^4$ cells/well in culture medium. Serial dilutions of mouse or human TNF (mTNF or hTNF; Peprotech, Rocky Hill, NJ), anti-mFas antibody (clone Jo2; BD Biosciences), or paraformaldehyde-fixed tmTNF-Mφ were prepared with DMEM containing 1 μg/ml cycloheximide, and added to each well. After 48 h incubation, the cell viability was measured by WST-8 assay kit (Nacalai Tesque) according to the manufacturer's instructions. The assay is based on cleavage of the tetrazolium salt WST-8 to formazan by cellular mitochondrial dehydrogenase.

### 2.6. Induction of GM-CSF secretion on PC60-hR2

$5 \times 10^4$ of PC60-hR2 cells were seeded on a 96 well plate and then exposed to a serial dilution of hTNF in the presence of IL-1β (2 ng/ml). After 24 h incubation, hTNFR2-mediated GM-CSF secretion on PC60-hR2 cells was quantified by ELISA kit according to the manufacturer's protocol (R&D Systems, Minneapolis, MN).

### 2.7. Immunoprecipitation and western blotting

For immunoprecipitation we used FLAG-TNF (a FLAG-tag fusion protein of hTNF), which was generated in *E. coli* and purified in our laboratory. The protocol for the expression and purification of recombinant proteins has been described previously (Yamamoto et al., 2003). $1 \times 10^7$ hTNFR2/mFas-PA cells were treated with or without 100 ng/ml of FLAG-TNF for 30 min at 37 °C. Cells were then harvested and lysed in 1 ml of lysis buffer (50 mM Tris HCl, pH 7.4, 150 mM NaCl, 1% Triton X-100, 1 mM EDTA and protease inhibitor cocktail; Sigma-Aldrich Inc.) and gently rocked at 4 °C for 30 min. Cell debris was removed by centrifugation at 10,000 ×g for 30 min. The resulting supernatant was immunoprecipitated with anti-FLAG-M2 affinity beads (Sigma, St.Louis, MO) for 4 h at 4 °C. Immune complexes bound to the beads were washed three

times with 500 μl of lysis buffer and eluted with 3×FLAG peptide at a concentration of 150 ng/ml. Collected proteins were resolved on 10–20% SDS-PAGE gels and transferred to polyvinylidene fluoride membranes (Millipore Corp., Billerica, MA) by electroblotting. Western blot analyses were performed with biotinylated anti-hTNFR2 antibody (R&D systems) or anti-FADD (Fas-associated death domain protein) antibody (H-181; Santa Cruz Biotechnology Inc., Santa Cruz, CA). Bound primary antibodies were visualized with horseradish peroxidase-conjugated streptavidin or goat–anti-rabbit-IgG (Jackson Immunoresearch Lab., West Grove, PA) respectively, and ECL plus western blotting detection reagents (GE Healthcare, Buckinghamshire, UK). A LAS 3000 image analyzer (Fujifilm, Tokyo, Japan) was used for the observation of chemiluminescence.

## 3. Results

### 3.1. Fas- but not TNFR-mediates induction of cell-death in $TNFR1^{-/-}R2^{-/-}$ preadipocytes

Initially, we established a cell line that could be used to evaluate TNFR2-specific bioactivity by means of the chimeric receptor (hTNFR2/mFas) strategy. The parental cell line must

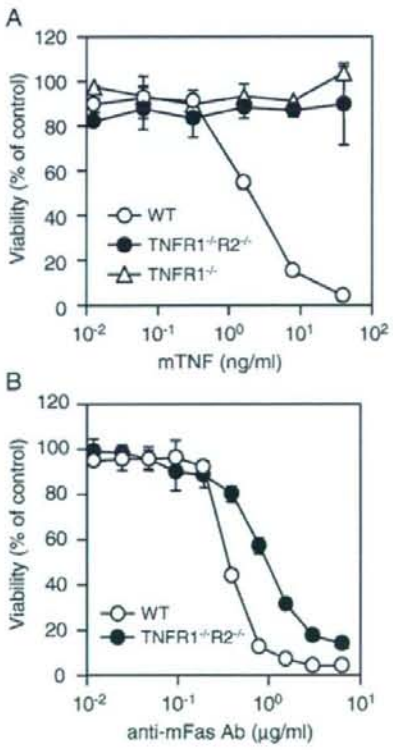


**Fig. 2.** Fas, but not TNFR2, induced cell death in preadipocytes. WT, $TNFR1^{-/-}$ $R2^{-/-}$ and $TNFR1^{-/-}$ cells were treated with serial dilutions of (A) mTNF or (B) anti-mFas Ab. Cell viability was determined using the WST-8 Assay. Each data point represents the mean±SD of triplicate wells.

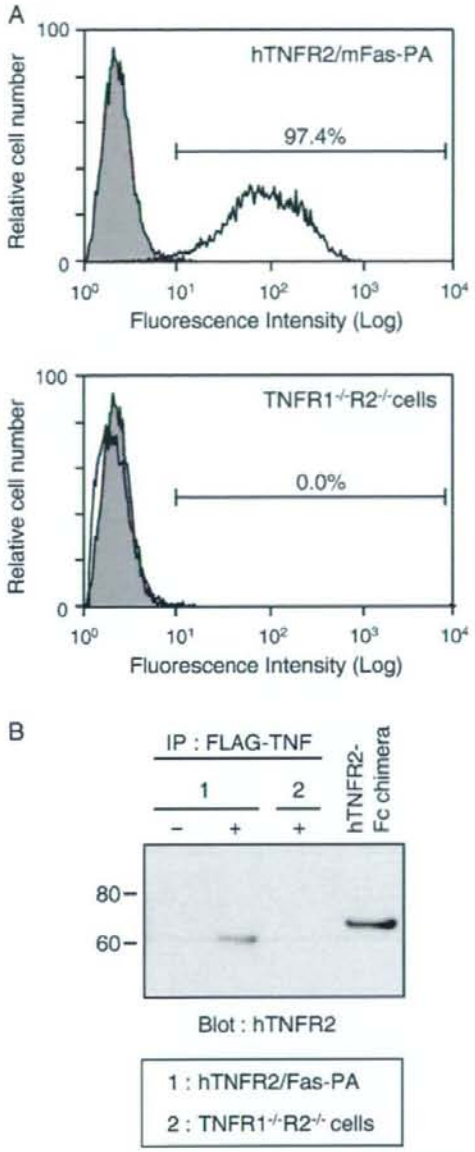


**Fig. 3.** Expression of hTNF2/mFas chimeric receptor on transfectants. (A) Expression of the chimeric receptor on hTNFR2/mFas-PA (upper panel) or parental $TNFR1^{-/-}R2^{-/-}$ cells (lower panel) was analyzed by flow cytometry using hTNFR2-specific antibody (open histograms) or isotype control antibody (shaded histograms). (B) hTNFR2/mFas-PA or $TNFR1^{-/-}R2^{-/-}$ cells were treated (+) with FLAG-TNF; (−) denotes untreated control cells. Immunoprecipitation was performed with anti-FLAG antibody M2-conjugated beads. After extensive washing, the immunocomplexes were eluted with 3×FLAG peptide. Eluted proteins were resolved on 10–20% SDS-PAGE gels and the presence of hTNFR2/mFas in the complex was detected by western blot using anti-hTNFR2 antibody.

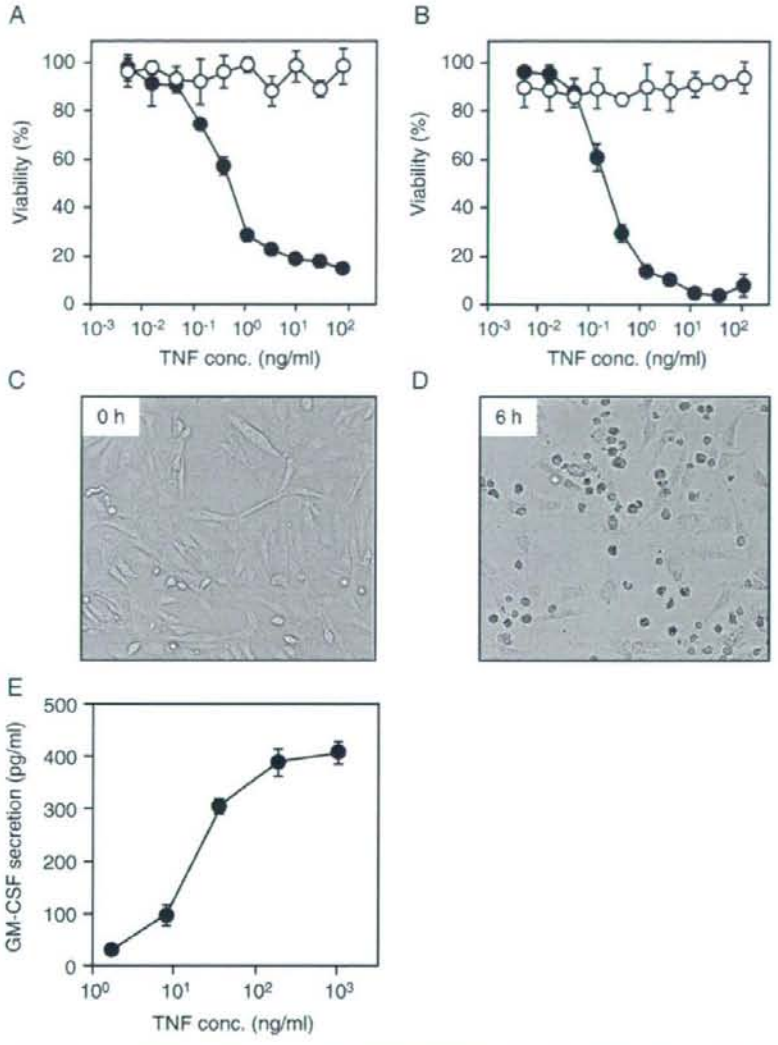


**Fig. 4.** Induction of strong cell death on hTNFR2/mFas-PA by soluble hTNF. hTNFR2/mFas-PA (●) and parental TNFR1$^{-/-}$R2$^{-/-}$ (○) cells were treated with serial dilutions of hTNF in the presence of cycloheximide (1 μg/ml). After (A) 24 h and (B) 48 h, the cell viability was measured using the WST-8 Assay. Data from the WST-8 assay represents the mean and SDs of triplicate assays. Similar results were obtained in three independent experiments. (C) Untreated or (D) hTNF-treated (10 ng/ml) hTNFR2/mFas-PA cells were incubated for 6 h, and were assessed by light microscopy. (E) PC60-hR2 cells were incubated in the presence of a serial dilution of hTNF and IL-1β (2 ng/ml). After 24 h, induction of GM-CSF was determined by ELISA. Each data point represents the mean ± SD of triplicate measurements.

possess both Fas-sensitivity and TNF-resistance. Thus, we selected TNFR1$^{-/-}$R2$^{-/-}$ preadipocytes as the parental cell line and then examined the susceptibility of this cell line against TNFR1- and Fas-induced cell death. TNFR1$^{-/-}$R2$^{-/-}$ preadipocytes were resistant to TNF-induced cell death, while WT preadipocytes, which co-express both TNFR1 and TNFR2, were killed by mTNF-treatment in a dose-dependent manner (Fig. 2A). TNFR1$^{-/-}$ preadipocytes were also resistant to TNF-induced cell death. Thus, TNF-mediated cell death is presumably due to TNFR1-stimuli in accordance with previous reports (Vandenabeele et al., 1995; Ashkenazi and Dixit, 1998; Devin et al., 2000). Anti-Fas antibody treatment induced cell death for both WT, R1$^{-/-}$ and TNFR1$^{-/-}$R2$^{-/-}$ preadipocytes (Fig. 2B). Based on these results, we therefore selected TNFR1$^{-/-}$R2$^{-/-}$ preadipocytes for constructing an hTNFR2/mFas-expressing cell line.

### 3.2. hTNFR2-expression analysis of LV-hTNFR2/mFas-Bsd infected Bsd-resistant cells

Using the LV technique followed by Bsd selection, we established transfectants that stably expressed hTNFR2/mFas chimeric receptor in which the EC and TM portion of hTNFR2 (amino acids 1–292) was fused to the IC region of mFas (amino acids 187–328) (Figs. 1A and B). FCM analysis revealed that almost 95% of Bsd-resistant cells expressed the EC domain of hTNFR2 (Fig. 3A). To determine whether hTNFR2/mFas retained binding activity against hTNF, we next performed immunoprecipitation and western blot analysis (Fig. 3B). These analyses showed that FLAG-TNFs were immunoprecipitated and eluted with hTNFR2/mFas from LV-transfected and Bsd-resistant cells, but not from parental TNFR1$^{-/-}$R2$^{-/-}$ preadipocytes and untreated cells. Thus, we succeeded in constructing hTNFR2/mFas expressing TNFR1$^{-/-}$R2$^{-/-}$ preadipocytes that retained the ability to bind hTNF.

### 3.3. Induction of apoptosis on hTNFR2/mFas-PA

To examine whether the death signal could be transduced by stimulating the chimeric receptors, we evaluated the cell viability of soluble hTNF-treated hTNFR2/mFas-PA. As anticipated, addition of hTNF to hTNFR2/mFas-PA induced a strong cytotoxic effect 24 and 48 h later, whereas no cell death was detected using parental TNFR1$^{-/-}$R2$^{-/-}$ preadipocytes (Figs. 4A and B). After 48 h, more than 90% of hTNFR2/mFas-PA cells were killed by hTNF at a concentration of 4 ng/ml, resulting in a median effective concentration (EC50) of 250 pg/ml. The images in Figs. 4C and D show that hTNFR2/mFas-PA cells underwent clear morphological changes, indicating apoptosis by hTNF stimuli. Additionally, PC60-hR2 cells were tested for hTNFR2-mediated GM-CSF secretion (Fig. 4E). The concentration required to induce 50% of maximal secretion of GM-CSF obtained with hTNF (EC50) was approximately 20 ng/ml. Importantly, our bioassay based on cell death phenotype displayed a ~80-fold higher level of sensitivity over conventional methodologies. Moreover, tmTNF (Fig. 5) and anti-TNFR2 agonistic antibody (data not shown) induced hTNFR2/mFas-PA cell death.

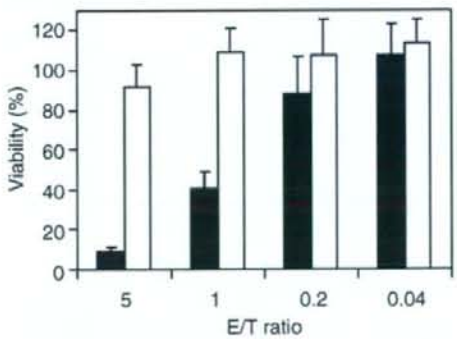


**Fig. 5.** hTNFR2/mFas-PA cells could be induced cell death by tmTNF. hTNFR2/mFas-PA cells were co-incubated with paraformaldehyde-fixed tmTNF-Mϕ (filled bars) or TNFR1$^{-/-}$R2$^{-/-}$ Mϕ (open bars) at an effector/target (E/T) ratio of 5:1, 1:1, 0.2:1 and 0.4:1 in the presence of cycloheximide (1 μg/ml). After 48 h, cell viability was measured by WST-8 Assay. Each data point represents the mean ± SD of triplicate measurements.

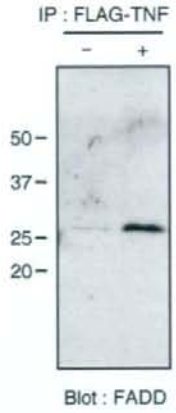


**Fig. 6.** Recruitment of FADD to the hTNFR2/mFas chimeric receptor in response to hTNF. hTNFR2/mFas-PA or TNFR1$^{-/-}$R2$^{-/-}$ cells were treated (+) with FLAG-TNF; (–) denotes untreated cells. Immunoprecipitation was performed with anti-FLAG antibody M2-conjugated beads. After extensive washing, immunocomplexes were eluted with 3×FLAG peptide. The eluted proteins were resolved on 10–20% SDS-PAGE gels and the presence of hTNFR2/mFas in the complex was detected by western blot using anti-FADD Antibody.

### 3.4. Recruitment of FADD to the hTNFR2/mFas chimeric receptor

Recent studies indicate that some TNFR family members, including Fas, self-associate as trimers prior to ligand binding. Activation of the pre-associated receptors is triggered by ligand-induced rearrangement of the assembled trimers (Algeciras-Schimnich et al., 2002). We speculated that the first reaction after ligand-induced oligomerization of hTNFR2/mFas might be the recruitment of FADD, leading to caspase-8 activation. To investigate the composition of the ligand-hTNFR2/mFas signaling complex, we treated hTNFR2/mFas-PA cells with FLAG-tagged hTNF and affinity purified the receptor complex using anti-FLAG antibody-conjugated beads, followed by western blot analysis with antibody against FADD. As expected, FADD was immunoprecipitated with hTNFR2/mFas on hTNF-treated hTNFR2/mFas-PA (Fig. 6). In similar experiments, we could not detect TRADD, which is recruited to TNFR1 in a ligand-dependent process (data not shown). It has been reported that, in contrast to TNFR1, Fas does not interact with TRADD but directly recruits FADD, leading to efficient cell death (Stanger et al., 1995; Dempsey et al., 2003). Because hTNFR2/mFas interacts with FADD, our hTNFR2/mFas-PA cell-based assay system will be useful for evaluating hTNF activity specifically *via* hTNFR2.

## 4. Discussion

Here, we developed a hTNFR2/mFas-PA cell-based assay system in order to investigate hTNF activity through hTNFR2. The assay is simple to perform and can detect hTNF-mediated hTNFR2 activity with high sensitivity. Because the hTNFR2/

mFas-PA system was engineered in TNFR1$^{-/-}$R2$^{-/-}$ preadipocytes, we were able to analyze hTNF-mediated hTNFR2 activity without affecting TNFR1-related apoptosis. Moreover, not only tmTNF- but also soluble TNF-mediated hTNFR2 activity was detectable using the hTNFR2/mFas-PA cell system.

In our system, hTNFR2-mediated cytotoxic activity on hTNFR2/mFas-PA cells was quantitatively determined using the WST-8 assay. Alternative methods, such as the MTT assay or Methylene Blue assay, are also capable of detecting cytotoxicity. Using the WST-8 assay, hTNFR2-mediated cytotoxic activity was readily detected 24 h after hTNF treatment (Fig. 4A), although a stronger signal was generated with a longer incubation time (48 h; Fig. 4B). Therefore, 48 h-treatment might be more appropriate for evaluating the activity of a low dose of hTNF or when analyzing an activity-weakened mutant TNF. Furthermore, if you evaluate in the absence of CHX, it may be desirable to alter the cell numbers from 1.5 to $1.0\times10^4$ cells/well. Previously, a similar assay system to the one described in this report was developed by Heidenreich et al. based on murine TNFR1$^{-/-}$R2$^{-/-}$ cells, which heterogenetically expressed human Fas conjugated with hTNFR2 (termed MF-R2-Fas cells) (Krippner-Heidenreich et al., 2002). However, there are some important differences between the MF-R2-Fas cells and the cell line used in our assay system (hTNFR2/mFas-PA), such as detachability. Surprisingly, unlike MF-R2-Fas cells, hTNFR2/mFas-PA cells can detect tmTNF-mediated activity as well as soluble TNF activity. Currently, the reason for this difference is unclear, although it may be caused by heterogeneity of the Fas domain. Indeed, the genetic homology between murine Fas and human Fas in IC domain is approximately 50%. Additionally, other factors may account for the observed differences between the two assay systems, such as expression level of the chimeric receptor. At any event, our results suggest that hTNFR2/mFas-PA cells will be useful in providing the basis for a highly sensitive assay system for analyzing hTNFR2 activity mediated by both soluble TNF and tmTNF. We are currently attempting to generate a TNFR2-selective mutant TNF using this assay system and a phage display system for TNF-therapy or anti-TNF therapy (unpublished data). We chose to use hTNFR2/mFas-PA cells in the screening process for a TNFR2-selective mutant TNF because this cell line is sensitive against not only purified TNF but also culture supernatants of TNF-transfected *E. coli* (crude samples). Therefore, our simple and sensitive bioassay enables high-throughput screening for TNFR2-selective mutant TNFs. The TNFR2-selective mutant will make it possible to perform a structure-function study of TNF/TNFR at any stage of function.

With the success of the human genome project, the focus of life science research has shifted to functional and structural analyses of proteins, such as disease proteomics (Oh et al., 2004; Gilchrist et al., 2006). Thus, there is increasing expectation on drug discovery/development based on the information from genomics or proteomics research, structural biology studies, or receptor-ligand interaction analyses. In particular, the therapeutic application of bioactive proteins, such as cytokines and the newly identified ligand proteins, is eagerly awaited (Gollob et al., 2003; Ansell et al., 2006). Surprisingly, however, these ligand proteins display multiple functions, which has severely limited their clinical application (Margolin et al., 1994; Eskander et al., 1997). Because the reason behind this limitation is that these ligand proteins stimulate different signal transduction pathways via multiple (two or more) receptors, the discovery of receptor-specific agonistic or antagonistic drugs is keenly awaited. Our assay system using a chimeric receptor strategy is applicable to other cytokines and thereby provides a new avenue for identifying receptor-specific agonists or antagonists. We fully anticipate that our novel technology will accelerate the development of TNFR2-related therapeutic molecules as well as acting as a research tool for studying the biology of TNFR2.

## Acknowledgements

This study was supported in part by Grants-in-Aid for Scientific Research (No. 18015055, 17689008) from the Ministry of Education, Culture, Sports, Science and Technology of Japan, in part by Health Labor Sciences Research Grant from the Ministry of Health, Labor and Welfare of Japan, in part by Health Sciences Research Grants for Research on Health Sciences focusing on Drug Innovation from the Japan Health Sciences Foundation, and in part by JSPS Research Fellowships for Young Scientists from the Japan Society for the Promotion of Science.

## References

Aggarwal, B.B., 2003. Signalling pathways of the TNF superfamily: a double-edged sword. Nat. Rev. Immunol. 3, 745.

Algeciras-Schimnich, A., Shen, L., Barnhart, B.C., Murmann, A.E., Burkhardt, J.K., Peter, M.E., 2002. Molecular ordering of the initial signaling events of CD95. Mol. Cell Biol. 22, 207.

Ansell, S.M., Geyer, S.M., Maurer, M.J., Kurtin, P.J., Micallef, I.N., Stella, P., Etzell, P., Novak, A.J., Erlichman, C., Witzig, T.E., 2006. Randomized phase II study of interleukin-12 in combination with rituximab in previously treated non-Hodgkin's lymphoma patients. Clin. Cancer Res. 12, 6056.

Ashkenazi, A., Dixit, V.M., 1998. Death receptors: signaling and modulation. Science 281, 1305.

Brown, S.L., Greene, M.H., Gershon, S.K., Edwards, E.T., Braun, M.M., 2002. Tumor necrosis factor antagonist therapy and lymphoma development: twenty-six cases reported to the Food and Drug Administration. Arthritis Rheum. 46, 3151.

Curtis, J.R., Patkar, N., Xie, A., Martin, C., Allison, J.J., Saag, M., Shatin, D., Saag, K.G., 2007. Risk of serious bacterial infections among rheumatoid arthritis patients exposed to tumor necrosis factor alpha antagonists. Arthritis Rheum. 56, 1125.

Dempsey, P.W., Doyle, S.E., He, J.Q., Cheng, G., 2003. The signaling adaptors and pathways activated by TNF superfamily. Cytokine Growth Factor Rev. 14, 193.

Devin, A., Cook, A., Lin, Y., Rodriguez, Y., Kelliher, M., Liu, Z., 2000. The distinct roles of TRAF2 and RIP in IKK activation by TNF-R1: TRAF2 recruits IKK to TNF-R1 while RIP mediates IKK activation. Immunity 12, 419.

Eskander, E.D., Harvey, H.A., Givant, E., Lipton, A., 1997. Phase I study combining tumor necrosis factor with interferon-alpha and interleukin-2. Am. J. Clin. Oncol. 20, 511.

Feldmann, M., Maini, R.N., 2003. Lasker Clinical Medical Research Award. TNF defined as a therapeutic target for rheumatoid arthritis and other autoimmune diseases. Nat. Med. 9, 1245.

Gilchrist, A., Au, C.E., Hiding, J., Bell, A.W., Fernandez-Rodriguez, J., Lesimple, S., Nagaya, H., Roy, L., Gosline, S.J., Hallett, M., Paiement, J., Kearney, R.E., Nilsson, T., Bergeron, J.J., 2006. Quantitative proteomics analysis of the secretory pathway. Cell 127, 1265.

Gollob, J.A., Veenstra, K.G., Parker, R.A., Mier, J.W., McDermott, D.F., Clancy, D., Tutin, L., Koon, H., Atkins, M.B., 2003. Phase I trial of concurrent twice-weekly recombinant human interleukin-12 plus low-dose IL-2 in patients with melanoma or renal cell carcinoma. J. Clin. Oncol. 21, 2564.

Heller, R.A., Song, K., Fan, N., Chang, D.J., 1992. The p70 tumor necrosis factor receptor mediates cytotoxicity. Cell 70, 47.

Jacobs, M., Togbe, D., Fremond, C., Samarina, A., Allie, N., Botha, T., Carlos, D., Parida, S.K., Grivennikov, S., Nedospasov, S., Monteiro, A., Le Bert, M.,